Journal of Inclusion Phenomena and Molecular Recognition in Chemistry **22:** 155–168, 1995.

X-Ray Crystallographic Studies and Molecular Calculations on 1 : 1 Inclusion Complexes of Cholic Acid with Acetophenone and Its Derivatives

MOTONARI SHIBAKAMI,* MASANORI TAMURA and AKIRA SEKIYA
National Institute of Materials and Chemical Research, 1-1 Higashi, Tsukuba, Ibaraki 305, Japan.

(Received in final form: 4 May 1995)

Abstract. Molecular calculations were applied to four channel-type inclusion complexes of cholic acid (CA) with acetophenone or its derivatives (3′-, 4′-fluoroacetophenone and 2′-chloroacetophenone). According to the calculated results, both the total and van der Waals interaction energies between channel and included guests depend on the channel form determined by the guest species. Similarly, the channel form is responsible for the dipole moment of the channel. Further examination of the results suggests that dipole–dipole interaction does not play an important role in the determination of the guest orientation.

Key words. Multimolecular inclusion complex, cholic acid, van der Waals interaction, dipole–dipole interaction.

Supplementary Data relating to this article are deposited with the British Library as Supplementary Publication No. SUP 82193 (26 pages).

1. Introduction

For the last few years, much attention has been paid to the inclusion phenomena of cholic acid (CA), a naturally occurring steroid, and its derivatives [1–10]. Of particular note is that the assembly pattern of CA molecules depends on the guest species [2]. For instance, CA molecules form a channel-type structure when they accommodate aromatic substances or a cyclic lactone [3–6], whereas a cage-type structure is formed if an alcohol molecule is used as guest [7–9]. Further examination of these X-ray results indicates that guest species notably affect the side chain conformation of CA. Such conformational changes are particularly observed in the channel-type structures [10]. Thus the channel structures hitherto elucidated can be classified into two categories based on the conformation.

For a further understanding of the inclusion phenomena, we calculated the interaction energies between channel and included guest molecules in two kinds of channel structures. Here acetophenone (AP) and its derivatives [3′-, 4′-

* Author for correspondence.

fluoroacetophenone and 2′-chloroacetophenone (3′-FAP, 4′-FAP and 2′-ClAP, respectively)] are used as guest molecules. AP and 4′-FAP yield a similar channel-type structure, whereas 3′- and 4′-FAP adopt another type. In this paper we report a significant role of the channel structure on the host–guest interaction.

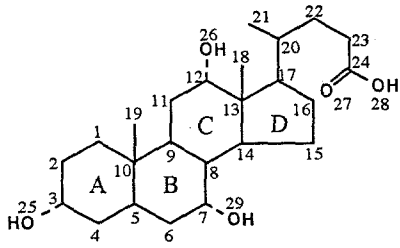

Cholic acid

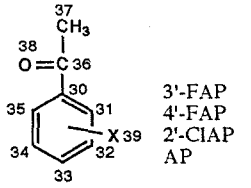

3'-FAP	X=F at *m*-position
4'-FAP	X=F at *p*-position
2'-ClAP	X=Cl at *o*-position
AP	X=H

2. Experimental

2.1. PREPARATION OF INCLUSION COMPLEXES

A solution of CA (0.3 g) in halogenated acetophenone (3′-, 4′-FAP and 2′-ClAP) (2 mL) was kept at room temperature for about 12 h and crystals of the inclusion complex with a host–guest ratio of 1 : 1 were obtained as colorless needles.

2.2. STRUCTURE ANALYSES AND REFINEMENT

Diffraction measurements were performed on a Rigaku AFC7R diffractometer with graphite monochromated CuK_α (λ = 1.54178 Å) radiation at 293 K. The data were corrected for Lorentz and polarization effects. An empirical absorption correction was applied using the program DIFABS [11]. A correction for secondary extinction was applied. The structures were solved by the direct methods: SHELXS86 [12] and DIRDIF92 [13]. Hydroxyl hydrogen atoms were located from the difference Fourier map. Hydrogen atoms except for hydroxyl hydrogen atoms were placed at calculated positions. Non-hydrogen atoms were refined anisotropically, whereas hydrogen atoms were included but not refined. The final cycle of full-matrix least-squares refinement was based on observed reflections [$I > 3.00\sigma(I)$]. The function minimized was $\sum w(|F_o|^2 - |F_c|^2)^2$. The weighting scheme used was $w = 1/\sigma^2(F_o) = 4F_o^2/\sigma^2(F_o^2)$. The absolute configurations were conformed to a previously reported structure of CA [3]. All calculations were performed using the TEXSAN crystallographic software package [14].

TABLE I. Crystal data and measurement conditions for CA inclusion complexes.

Complex	CA–3′-FAP	CA–4′-FAP	CA–2′-ClAP
Mol. formula	$C_{32}H_{47}FO_6$	$C_{32}H_{47}FO_6$	$C_{32}H_{47}ClO_6$
M	546.72	546.72	563.17
Space group	$P2_1$	$P2_1$	$P2_1$
Z	2	2	2
a/Å	12.794(4)	13.540(3)	12.580(2)
b/Å	7.813(4)	8.154(3)	7.984(2)
c/Å	16.172(4)	14.353(3)	16.045(2)
β/°	113.13(2)	113.27(1)	112.229(9)
V/Å^3	1485.7(9)	1455.8(7)	1491.8(4)
D_{calc}/g cm^{-3}	1.222	1.247	1.254
μ/cm^{-1}	6.71	6.85	14.63
Crystal size/mm	0.10 × 0.05 × 0.10	0.20 × 0.05 × 0.30	0.10 × 0.08 × 0.30
θ limit/°	120.2	120.1	120.2
No. of observed reflections (N_0)	1169	1518	1046
No. of variables (N_v)	352	352	352
R, R_w, GOF[a]	0.046, 0.050, 1.39	0.052, 0.058, 1.98	0.049, 0.024, 1.57

[a]GOF = $[\sum w(|F_o| - |F_c|)^2/(N_o - N_v)]^{1/2}$, where $w = 1/\sigma^2(F_o)$.

2.3. MOLECULAR MECHANICS CALCULATIONS

Molecular mechanics calculations were made with the CAChe™ Mechanics program of CAChe Scientific, Inc. on a Macintosh Quadra 950. The program can deal with up to about 4000 atoms, so that this program is sufficient for our host–guest model systems mentioned below. Our calculations did not take into account solvent molecules, i.e. acetophenone or its derivatives, because of the limitation of the program. The positional parameters of non-hydrogen atoms and methine, methylene and methyl hydrogen atoms were obtained from the X-ray results. The H atoms participating in a hydrogen bond were positioned as: (1) O—H distance is 1.00 Å, (2) O—H···O′ angle is 180.0°. The bifurcated hydrogen bond in CA–4′-FAP was also taken into account for positioning.

2.4. VAN DER WAALS SURFACE AREA, MOLECULAR VOLUME AND DIPOLE MOMENT CALCULATIONS

The dipole moments of the channels and the stacked guests were calculated by the PM3 method [15]. The positional parameters were the same as those for the MM calculations. All calculations were performed with the MOL-MOLIS/CRYS of Daikin Industries Co., Ltd. on an IRIS Indigo R4000 XS24 workstation by Silicon Graphics.

TABLE II. Positional parameters and temperature factors [$B_{(eq)}$] for non-hydrogen atoms of CA–3′-FAP.

Atom	x	y	z	$B_{(eq)}$ [a]
F(39)	0.0637(9)	−0.2056	0.7084(8)	15.3(5)
O(25)	0.4889(6)	−0.177(1)	1.0965(4)	5.1(2)
O(26)	0.5942(5)	0.136(1)	0.7894(3)	3.6(2)
O(27)	0.5190(6)	−0.093(1)	0.3254(4)	4.8(2)
O(28)	0.5335(5)	0.159(1)	0.2685(4)	4.5(2)
O(29)	0.6381(4)	−0.414(1)	0.8888(3)	3.7(2)
O(38)	0.124(1)	0.465(2)	0.5616(10)	15.7(5)
C(1)	0.7540(9)	0.041(2)	1.1034(6)	4.5(3)
C(2)	0.6271(8)	0.021(2)	1.0883(6)	4.1(3)
C(3)	0.6107(9)	−0.155(2)	1.1176(5)	4.4(3)
C(4)	0.6491(8)	−0.289(2)	1.0706(5)	3.7(3)
C(5)	0.7737(8)	−0.269(2)	1.0811(6)	3.5(3)
C(6)	0.8061(7)	−0.412(2)	1.0310(6)	3.5(2)
C(7)	0.7592(7)	−0.390(2)	0.9303(5)	3.1(2)
C(8)	0.7855(7)	−0.209(2)	0.9047(5)	3.1(2)
C(9)	0.7488(7)	−0.069(2)	0.9524(6)	3.2(2)
C(10)	0.8003(7)	−0.090(2)	1.0573(5)	3.1(2)
C(11)	0.7706(7)	0.106(2)	0.9195(5)	3.5(2)
C(12)	0.7163(7)	0.128(2)	0.8173(5)	2.9(2)
C(13)	0.7548(7)	−0.010(2)	0.7696(5)	3.1(3)
C(14)	0.7304(7)	−0.181(2)	0.8031(5)	2.8(2)
C(15)	0.7492(7)	−0.314(2)	0.7420(5)	3.4(2)
C(16)	0.7074(7)	−0.225(2)	0.6517(6)	3.7(3)
C(17)	0.6833(6)	−0.036(2)	0.6648(5)	2.9(2)
C(18)	0.8798(7)	0.016(2)	0.7885(5)	3.7(2)
C(19)	0.9310(8)	−0.063(2)	1.0952(5)	5.0(3)
C(20)	0.7032(7)	0.083(2)	0.5980(5)	2.8(2)
C(21)	0.6927(8)	0.272(2)	0.6133(6)	4.0(3)
C(22)	0.6182(7)	0.029(2)	0.5025(5)	4.3(3)
C(23)	0.6294(7)	0.123(2)	0.4248(5)	3.7(2)
C(24)	0.5538(7)	0.050(2)	0.3353(6)	3.3(3)
C(30)	0.133(1)	0.195(2)	0.6296(8)	5.7(4)
C(31)	0.0704(10)	0.069(3)	0.6521(8)	6.7(4)
C(32)	0.126(1)	−0.076(2)	0.689(1)	8.0(5)
C(33)	0.234(2)	−0.108(3)	0.7044(10)	10.3(6)
C(34)	0.292(1)	0.014(3)	0.679(1)	8.6(5)
C(35)	0.244(1)	0.173(3)	0.644(1)	8.7(5)
C(36)	0.077(1)	0.356(3)	0.5898(10)	8.4(5)
C(37)	−0.044(1)	0.390(2)	0.5751(10)	10.8(5)

[a] $B_{(eq)} = (8/3)\pi^2\{U_{11}(aa^*)^2 + U_{22}(bb^*)^2 + U_{33}(cc^*)^2 + 2U_{12}aa^*bb^* \cos\gamma + 2U_{13}aa^*cc^* \cos\beta + 2U_{23}bb^*cc^* \cos\alpha\}$.

TABLE III. Positional parameters and temperature factors [$B_{(eq)}$] for non-hydrogen atoms of CA–4′-FAP.

Atom	x	y	z	$B_{(eq)}$ [a]
F(39)	0.4154(6)	0.1196	0.3383(4)	11.8(3)
O(25)	−0.0935(4)	−0.080(1)	−0.1196(3)	4.9(1)
O(26)	0.1743(4)	0.224(1)	0.2966(3)	4.2(1)
O(27)	0.6551(8)	−0.027(2)	0.6654(9)	13.7(4)
O(28)	0.6922(5)	0.227(1)	0.6817(5)	7.7(2)
O(29)	0.0921(3)	−0.307(1)	0.2271(3)	3.8(1)
O(38)	0.3301(6)	−0.053(1)	−0.1112(5)	8.1(2)
C(1)	−0.1842(5)	0.103(1)	0.0735(5)	4.1(2)
C(2)	−0.1319(5)	0.094(1)	−0.0031(5)	3.6(2)
C(3)	−0.1458(6)	−0.074(1)	−0.0492(5)	4.0(2)
C(4)	−0.0990(6)	−0.201(1)	0.0329(5)	3.6(2)
C(5)	−0.1479(5)	−0.194(1)	0.1124(5)	3.6(2)
C(6)	−0.0996(6)	−0.327(1)	0.1940(5)	4.1(2)
C(7)	0.0132(5)	−0.292(1)	0.2709(5)	3.7(2)
C(8)	0.0194(5)	−0.121(1)	0.3153(5)	3.2(2)
C(9)	−0.0236(5)	0.011(1)	0.2333(5)	3.0(2)
C(10)	−0.1406(5)	−0.023(1)	0.1603(5)	3.3(2)
C(11)	−0.0058(6)	0.183(1)	0.2805(5)	3.6(2)
C(12)	0.1094(5)	0.220(1)	0.3550(5)	3.4(2)
C(13)	0.1492(5)	0.090(1)	0.4393(4)	3.0(2)
C(14)	0.1341(5)	−0.078(1)	0.3881(5)	2.9(2)
C(15)	0.1900(6)	−0.196(1)	0.4768(5)	4.2(2)
C(16)	0.2872(6)	−0.098(1)	0.5476(5)	3.6(2)
C(17)	0.2718(5)	0.081(1)	0.5072(5)	3.2(2)
C(18)	−0.2190(6)	−0.013(2)	0.2159(6)	5.6(2)
C(19)	0.0849(6)	0.108(1)	0.5078(5)	4.3(2)
C(20)	0.3244(6)	0.206(1)	0.5938(5)	4.2(2)
C(21)	0.3083(7)	0.383(1)	0.5595(7)	6.0(3)
C(22)	0.4450(6)	0.163(1)	0.6538(5)	4.9(2)
C(23)	0.5121(6)	0.163(2)	0.5920(6)	5.6(2)
C(24)	0.6252(7)	0.113(2)	0.6527(7)	5.9(2)
C(30)	0.4064(6)	0.065(1)	0.0536(6)	4.3(2)
C(31)	0.3236(7)	0.005(1)	0.0787(7)	5.6(2)
C(32)	0.3272(8)	0.024(2)	0.1755(8)	6.7(3)
C(33)	0.4071(9)	0.107(2)	0.2408(7)	7.0(3)
C(34)	0.4917(8)	0.167(2)	0.2214(8)	7.2(3)
C(35)	0.4873(6)	0.149(1)	0.1255(7)	5.6(2)
C(36)	0.3998(7)	0.034(2)	−0.0510(7)	5.8(3)
C(37)	0.4777(9)	0.116(2)	−0.0837(7)	10.2(4)

[a] $B_{(eq)} = (8/3)\pi^2\{U_{11}(aa^*)^2 + U_{22}(bb^*)^2 + U_{33}(cc^*)^2 + 2U_{12}aa^*bb^* \cos\gamma + 2U_{13}aa^*cc^* \cos\beta + 2U_{23}bb^*cc^* \cos\alpha\}$.

TABLE IV. Positional parameters and temperature factors [$B_{(eq)}$] for non-hydrogen atoms of CA–2′-ClAP.

Atom	x	y	z	B_{eq} [a]
Cl(39)	1.0443(3)	0.5523	0.1692(2)	7.6(1)
O(25)	0.4821(7)	0.626(1)	0.5952(5)	5.3(3)
O(26)	0.5970(6)	0.933(1)	0.2924(4)	3.4(2)
O(27)	0.5198(8)	0.693(1)	−0.1783(6)	5.7(3)
O(28)	0.5274(7)	0.950(1)	−0.2309(5)	5.3(3)
O(29)	0.6384(6)	0.387(1)	0.3874(4)	3.3(2)
O(38)	0.9111(7)	0.727(2)	−0.0108(6)	8.3(4)
C(1)	0.755(1)	0.833(2)	0.6057(7)	4.4(4)
C(2)	0.628(1)	0.817(2)	0.5885(7)	4.6(4)
C(3)	0.605(1)	0.643(2)	0.6192(7)	3.6(4)
C(4)	0.648(1)	0.513(2)	0.5709(7)	3.8(4)
C(5)	0.7733(10)	0.529(2)	0.5823(7)	3.0(4)
C(6)	0.8080(9)	0.393(2)	0.5316(8)	4.0(4)
C(7)	0.7612(10)	0.414(2)	0.4295(7)	3.3(4)
C(8)	0.7867(9)	0.591(2)	0.4034(7)	2.6(3)
C(9)	0.7512(9)	0.730(2)	0.4529(6)	2.3(3)
C(10)	0.8011(9)	0.706(2)	0.5580(7)	2.8(3)
C(11)	0.7770(9)	0.900(2)	0.4207(7)	3.1(3)
C(12)	0.7220(9)	0.924(1)	0.3178(7)	3.0(3)
C(13)	0.7568(8)	0.784(2)	0.2687(6)	2.3(3)
C(14)	0.7322(9)	0.619(2)	0.3030(7)	2.4(3)
C(15)	0.7507(10)	0.488(1)	0.2402(7)	3.8(3)
C(16)	0.7062(10)	0.576(2)	0.1478(6)	3.4(3)
C(17)	0.6864(8)	0.765(2)	0.1656(7)	2.3(3)
C(18)	0.8831(8)	0.808(2)	0.2850(6)	3.5(3)
C(19)	0.9345(9)	0.732(2)	0.5937(6)	4.6(3)
C(20)	0.7033(9)	0.877(2)	0.0945(7)	3.1(3)
C(21)	0.694(1)	1.062(2)	0.1130(7)	4.8(4)
C(22)	0.6184(8)	0.827(2)	0.0008(7)	4.1(3)
C(23)	0.6402(10)	0.900(2)	−0.0773(7)	4.6(4)
C(24)	0.557(1)	0.830(2)	−0.1674(9)	4.0(4)
C(30)	1.112(1)	0.728(2)	0.0540(9)	4.4(4)
C(31)	1.138(1)	0.674(2)	0.1412(10)	4.3(4)
C(32)	1.243(1)	0.714(2)	0.210(1)	6.6(5)
C(33)	1.317(1)	0.813(3)	0.187(1)	7.7(6)
C(34)	1.296(1)	0.867(2)	0.102(1)	6.7(5)
C(35)	1.191(1)	0.826(2)	0.0363(9)	5.8(5)
C(36)	0.998(1)	0.691(2)	−0.0215(9)	5.7(5)
C(37)	0.995(1)	0.621(2)	−0.1066(8)	7.4(5)

[a] $B_{(eq)} = (8/3)\pi^2\{U_{11}(aa^*)^2 + U_{22}(bb^*)^2 + U_{33}(cc^*)^2 + 2U_{12}aa^*bb^* \cos\gamma + 2U_{13}aa^*cc^* \cos\beta + 2U_{23}bb^*cc^* \cos\alpha\}$.

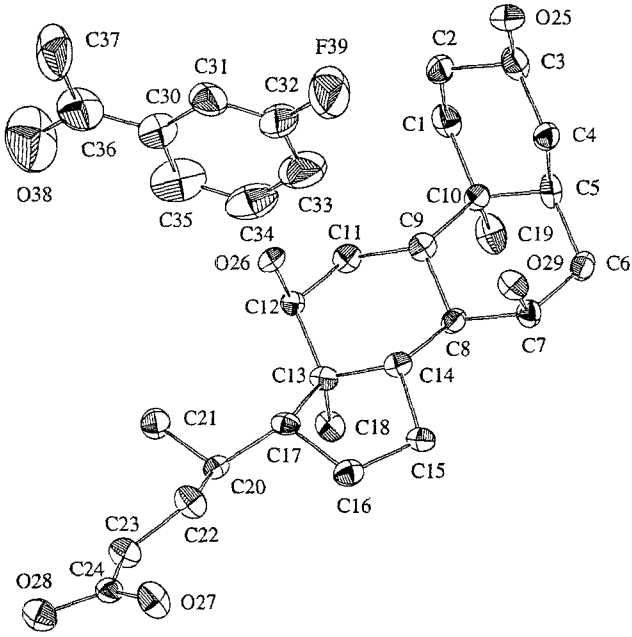

Fig. 1. ORTEP drawing of the molecular structures of CA and 3′-FAP in CA–3′-FAP inclusion complex. All the atoms are represented by thermal ellipsoids with 30% probability levels. H atoms are omitted for clarity.

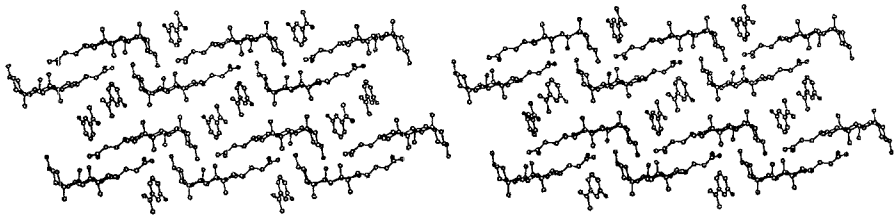

Fig. 2. Stereodrawing of CA–3′-FAP inclusion complex as viewed along the crystallographic *b*-axis. H atoms are omitted for clarity.

3. Results and Discussion

3.1. CRYSTAL STRUCTURE OF INCLUSION COMPLEXES

The measurement conditions and structural details are listed in Table I. The positional parameters and temperature factors for non-hydrogen atoms are given in Tables II, III and IV. Figure 1 shows ORTEP [16] drawings of CA and 3′-FAP. The crystal structures drawn by CHARON [17] of CA–3′-FAP, –4′-FAP, –2′-CIAP and –AP are depicted in Figures 2 and 3. CA molecules are arranged to form an amphiphilic layered structure. These layered structures provide channel-like spaces in the hydrophobic layers just along the *b*-axis, and the guest molecules are

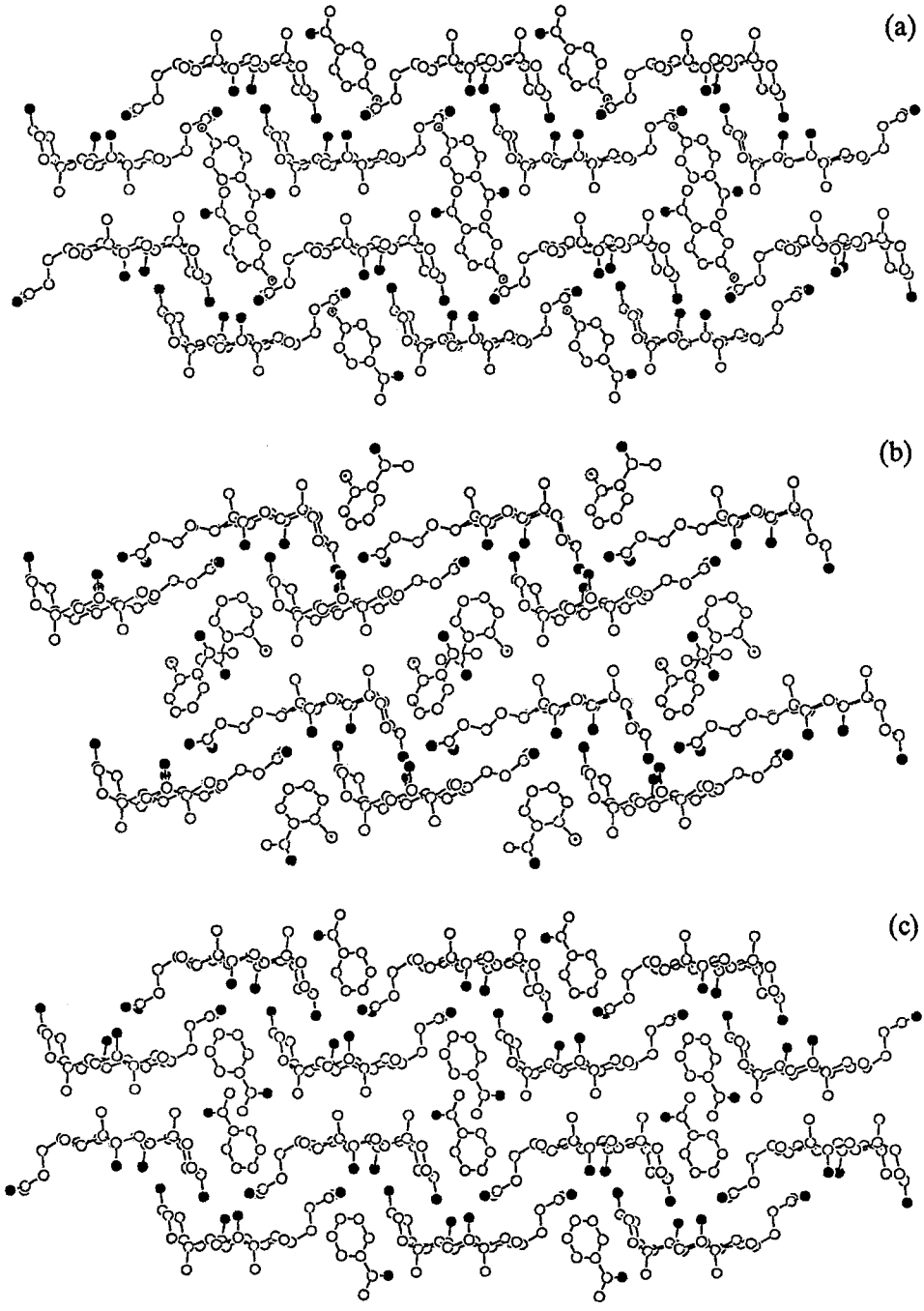

Fig. 3. CHARON drawings of the packing diagrams of the CA inclusion complexes as viewed along the *b*-axis: (a) CA–4′-FAP, (b) CA–2′-ClAP, (c) CA–AP [3]. C, O and F atoms are represented by empty, filled and half-filled circles, respectively. H atoms are omitted for clarity.

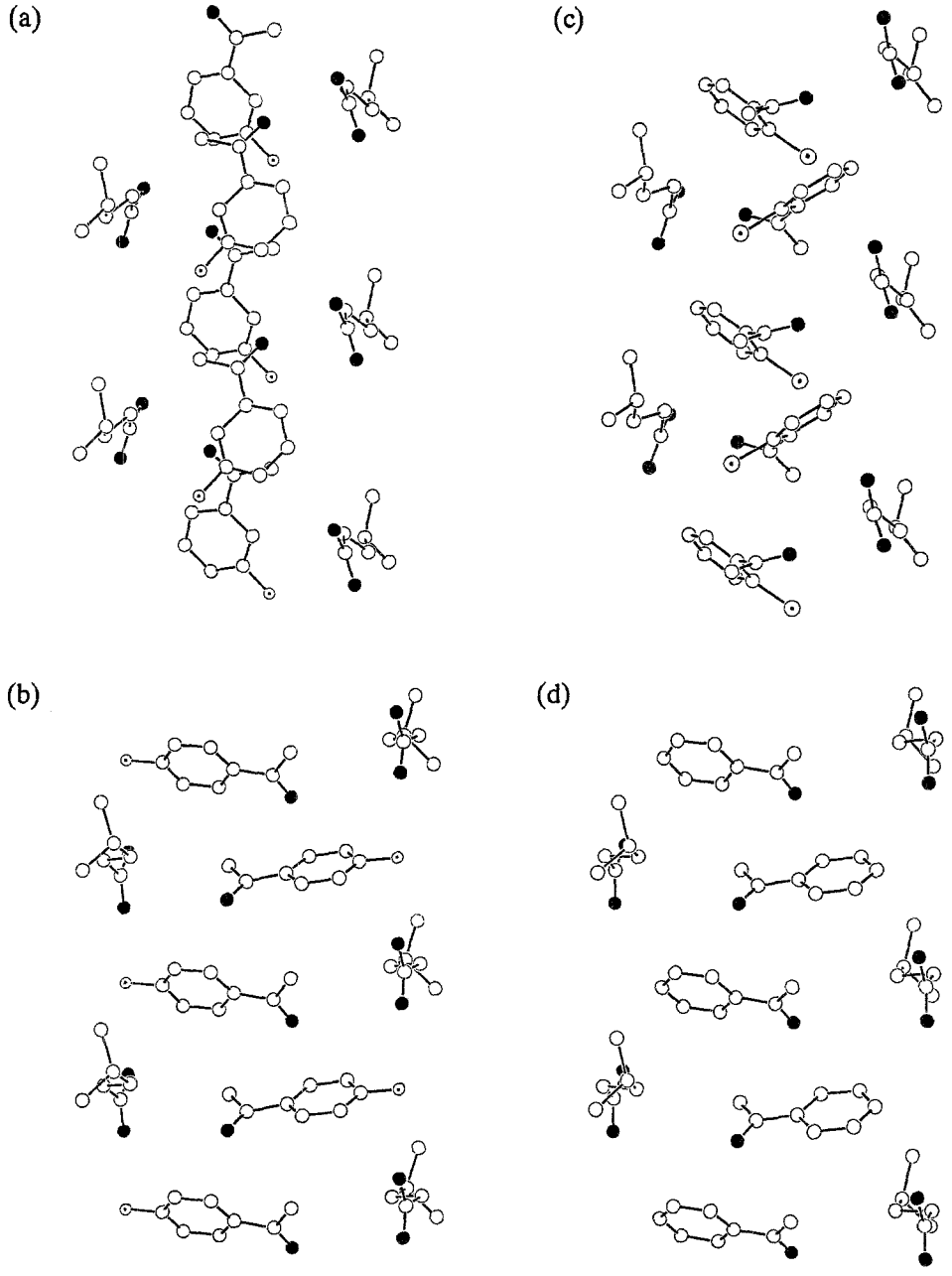

Fig. 4. Schematic drawings of the channels of CA including guests. The channel walls are represented as the steroidal side chains; (a) CA–3′-FAP, (b) CA–4′-FAP, (c) CA–2′-ClAP and (d) CA–AP [3]. C, O and F (Cl) atoms are represented by empty, filled and half-filled circles, respectively. H atoms are omitted for clarity.

tightly accommodated inside the channels. Differences in guest orientation are found among the structures. The phenyl planes of 4′-FAP and AP point toward the side chain of CA, while those of 3′-FAP and 2′-ClAP are directed to the steroidal A ring. The channels are shown in Figure 4. 3′-FAP and 2′-ClAP molecules are accommodated in the channel so that their phenyl planes are nearly parallel to the channel direction, while the planes of 4′-FAP and AP are nearly perpendicular to this direction.

As Figures 2 and 3 show, there are two kinds of channels in which CA molecules accommodate the given guests. One consists of the A, C and D rings and the side chains with the C(17)—C(20)—C(22)—C(23) dihedral angle (ψ) of the *trans* conformation as observed in CA–3′-FAP and –2′-ClAP: the ψ angles are $-175.6(7)$ and $-167.7(10)°$, respectively, whereas the other consists of the A and C rings and the side chains with *gauche* in CA–4′-FAP and –AP: the ψ angles are 59.7(9) and 58.3(5)°, respectively. The former and the latter are hereafter referred to as channel type I and type II, respectively.

As previously reported, the cyclic hydrogen bond network with a sequence of —O(26)—H· · · O(27)=C(24)—O(28)—H· · · O(29)—H· · · O(25)—H· · · O(26) plays an important role in the stabilization of the molecular assembly in the CA–AP crystal structure [3]. The same network is observed in the CA–3′-FAP, –4′-FAP and –2′-ClAP structures. In addition to this network, a hydrogen bond (or at least a weak interaction) between F(39) and O(26) atoms with a distance of 3.195(9) Å is found in the CA–4′-FAP structure. The large $B_{(eq)}$ of O(27) [13.7(4) Å^2] suggests that the O(26)· · ·O(27) bond is somewhat broken by the F(39)· · ·O(26) interaction. Such a bifurcated hydrogen bond cannot be observed in the other structures.

3.2. MOLECULAR MECHANICS CALCULATIONS

Figure 5 shows the host-guest model system of CA–3′-FAP for molecular mechanics calculation. This system consists of eighteen hosts and six stacked guests. Similar systems were used for the other complexes. The interaction between channel and included guests was evaluated as the energy difference between [(energy of the host lattice) + (energy of the stacked guests)] and [total energy of the model system]. The total interaction energies (ΔE^i), together with values of $\Delta E^i_{\mathrm{vdW}}$, a van der Waals interaction term, are given in Table V. All the values are negative, which agree with the notion that the present complexes are formed and van der Waals interaction generally contributes to the stabilization. Table V shows that channel type I accommodates the guest molecules more tightly than type II.

It has been established that van der Waals interaction dominates the stabilization of the molecular complex. Thus we further examined this term in order to understand the difference in the total interaction energy. In fact, the large difference in $\Delta E^i_{\mathrm{vdW}}$ suggests that the ΔE^i difference results from the disparity in van der Waals interaction. It is well known that van der Waals interaction arises from the sum of London dispersion forces between all non-bonded atom pairs in a molecular com-

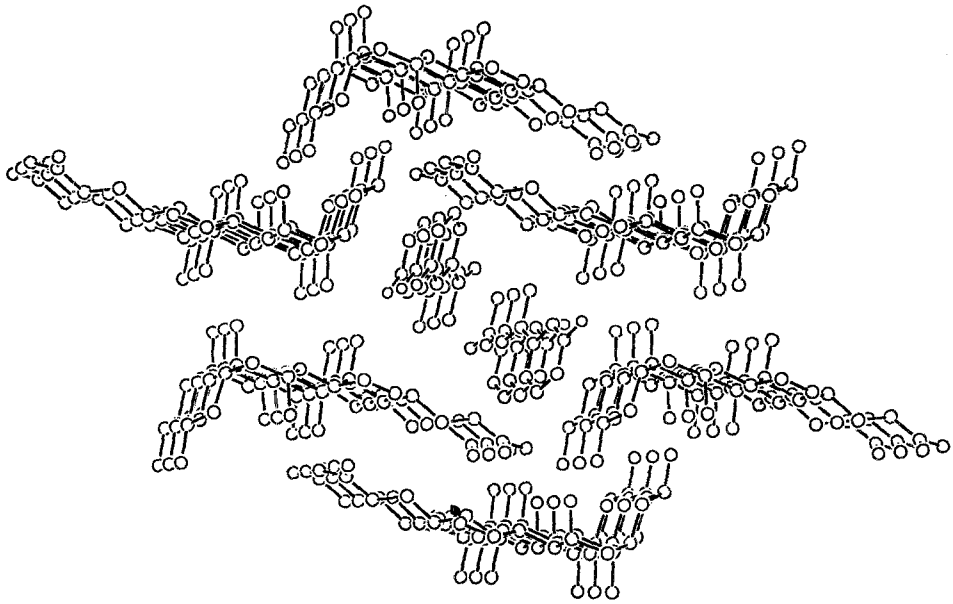

Fig. 5. Schematic drawing of the host-guest model system of CA–3′-FAP viewed down the *b*-axis. H atoms are omitted for clarity.

TABLE V. Total and van der Waals interaction energies between the channel and the included stacked guests (ΔE^i and $\Delta E^i_{\mathrm{vdW}}$, respectively) (in kcal mol^{-1}).

Complex	ΔE^i	$\Delta E^i_{\mathrm{vdW}}$
CA–3′-FAP	−101.5	−91.6
CA–4′-FAP	−131.3	−113.0
CA–2′-ClAP	−116.0	−106.6
CA–AP	−119.8	−109.9

plex. Thus this interaction is ascribed essentially to the close proximity between the outer surface of the guest and the interior wall of the channel. From this theory, $\Delta E^i_{\mathrm{vdW}}$ values suggest that the wall of channel type I contacts guest molecules more widely than type II. To examine the relation between $\Delta E^i_{\mathrm{vdW}}$ values and guest size, we calculated the van der Waals surface area and the molecular volume of the guest molecules. The calculated values are tabulated in Table VI. Although the surface area and the volume of 3′-FAP are not so small when compared to those of the other guests, the $\Delta E^i_{\mathrm{vdW}}$ value is the smallest. In addition, the $\Delta E^i_{\mathrm{vdW}}$ value of CA–2′-ClAP is smaller than those of CA–4′-FAP and –AP, in spite of the largest size of 2′-ClAP. Consequently, these calculations suggest that the difference in the

TABLE VI. van der Waals surface areas (in Å^2) and molecular volumes (in Å^3) of the guests.

Guest	Surface area	Molecular volume
3′-FAP	119.0	150.8
4′-FAP	118.5	149.9
2′-ClAP	127.6	161.7
AP	115.0	145.5

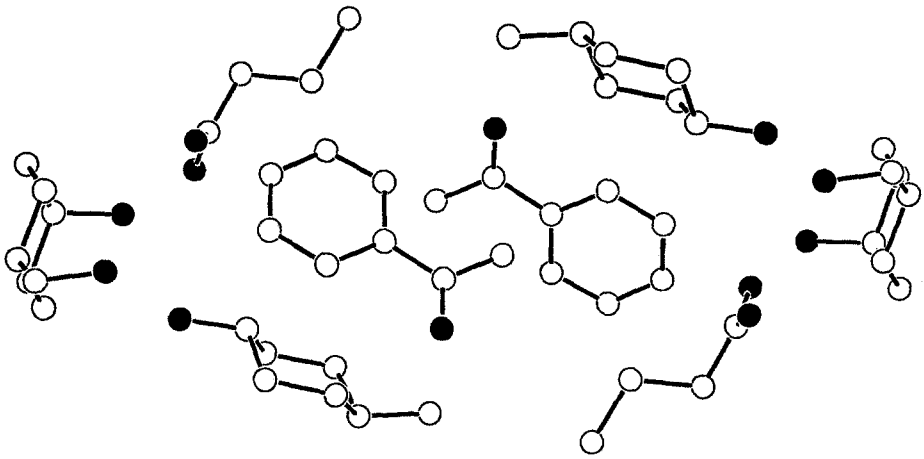

Fig. 6. Schematic drawing of two stacked AP and the corresponding channel moieties of the CA–AP inclusion complex. C and O atoms are represented by empty and filled circles, respectively. H atoms are omitted for clarity.

total energy results from the channel–guest contact mode based on the channel form, not from the guest size.

3.3. DIPOLE MOMENT CALCULATIONS

The dipole moments of the present channels were calculated. Figure 6 shows the model system of CA–AP for dipole moment calculation. This system consists of two stacked guests and the channel surrounding these guests. A similar system was applied to CA–4′-FAP. Another type of the system composed of two A, C and D rings and two side chains was used when the dipole moments of CA–3′-FAP and –2′-ClAP were calculated. It seems reasonable to suppose that the calculated moment agrees well with that of the actual channel, since these model systems contain all the polar groups in the channel. The calculated values are tabulated in Table VII, indicating that the dipole moment is an enormously large value in an infinitely long channel of the crystal. In other words, CA molecules aggregate to produce a large dipole moment. The dipole moment should be parallel to the *b*-axis, since the channel components are related by 2_1 symmetry. Table VII also

TABLE VII. Dipole moments of two stacked guests and the corresponding channel surrounding the guests (in D).

Complex	Dipole moment[a,b]	
	Channel	Stacked guests
CA–3′-FAP	−2.613	+1.744
CA–4′-FAP	−3.165	−2.917
CA–2′-ClAP	−2.144	+0.463
CA–AP	−3.001	−2.836

[a]Minus sign indicates that the moment direction runs from upside to down in Figure 4 and plus sign indicates the opposite direction.
[b]The calculated moments do not run exactly along the *b*-axis because of the finiteness in the models.

shows that channel type I has a larger moment than type II, which suggests that the conformation of the side chain affects the dipole moment.

We also calculated the dipole moments of two stacked guests in our model systems. The results are tabulated in Table VII. Our calculations show that several stacked guests have a large dipole moment comparable to the value for the channels. All the moments of the stacked guests are parallel to the *b*-axis because of the 2_1 symmetry relation between the guest molecules.

According to intermolecular interaction theory, long-range types of interaction, especially electrostatic interaction, should be primarily important for stabilizing non-covalent types of molecular complexes [18]. In addition, Kitagawa *et al.* previously reported that dipole–dipole interaction, the leading term of electrostatic interaction plays an important role in the determination of the guest orientation inside an α-cyclodextrin cavity [19]. Here we discuss the role of dipole-dipole interaction in the interaction between channel and guests. As shown in Table VII, the dipole moment directions of the channel are the same in all cases. In contrast, the moment directions of the stacked guests are inconsistent. That is, the dipole moments of the channel and the stacked guests run in the opposite direction to each other in CA–3′-FAP and –2′-ClAP, whereas they run in the same direction in CA–4′-FAP and –AP. Generally, the antiparallel relationship between two dipole moments are energetically more favorable than the parallel one. Thus the relationship observed in the former may indicate the important role of dipole–dipole interaction in stabilizing the complexes and/or determining the guest orientation in channel type II. The inconsistency of the relationship among the given complexes, however, shows that electrostatic interaction, mainly dipole–dipole interaction does not necessarily play an important role at least in the given channel-type complexes.

4. Conclusion

Using a series of molecules as guests, we have found that the van der Waals and dipole–dipole interactions between the channel and the guests depend on the channel form, i.e., the molecular assembly pattern. The results also indicate that the dipole–dipole interaction does not contribute to the complex stabilization, unlike the van der Waals interaction.

References

1. For example, Y. Cheng, D. M. Ho, C. R. Gottlieb, and D. Kahne: *J. Am. Chem. Soc.* **114**, 7319 (1992); K. Sada, T. Kondo, M. Miyata, T. Tamada, and K. Miki: *J. Chem. Soc., Chem. Commun.* 753 (1993); K. Sada, T. Kondo, M. Miyata, and K. Miki: *Chem. Mater.* **6**, 1103 (1994).
2. M. Miyata, M. Shibakami, S. Chirachanchai, K. Takemoto, N. Kasai, and K. Miki: *Nature (London)* **343**, 446 (1990).
3. K. Miki, A. Masui, N. Kasai, M. Miyata, M. Shibakami, and K. Takemoto: *J. Am. Chem. Soc.* **110**, 6594 (1988).
4. K. Miki, N. Kasai, M. Shibakami, K. Takemoto, and M. Miyata: *J. Chem. Soc., Chem. Commun.* 1757 (1991).
5. M. R. Caira, L. R. Nassimbeni, and J. L. Scott: *ibid.* 612 (1993).
6. M. Shibakami and A. Sekiya: *ibid.* 429 (1994).
7. P. L. Johnson and J. P. Schaefer: *Acta Crystallogr., Sect. B* **28**, 3083 (1972).
8. E. L. Jones and L. R. Nassimbeni: *ibid.* **46**, 399 (1990).
9. M. Shibakami and A. Sekiya: *J. Inclusion Phenom.* **18**, 397 (1994).
10. M. Miyata, K. Sada, K. Hirayama, Y. Yasuda, and K. Miki: *Supramol. Chem.* **2**, 283 (1993).
11. N. Walker and D. Stuart: 'DIFABS, An empirical absorption correction program', *Acta Crystallogr., Sect. A* **39**, 158 (1983).
12. G. M. Sheldrick: SHELXS86 in *Crystallographic Computing* 3, eds. G. M. Sheldrick, C. Cruger and R. Goddard, Oxford University Press, pp. 175–189 (1985).
13. P. T. Beurskens, G. Admiraal, G. Beurskens, W. P. Bosman, S. Garcia-Granada, R. O. Gould, J. M. M. Smits, and C. Smykalla: DIRDIF92, Technical Report of the Crystallography Laboratory, University of Nijmegen, The Netherlands (1992).
14. Molecular Structure Corporation: TEXSAN. TEXRAY Structure Analysis Package. MSC, 3200 Research Forest Drive, The Woodlands, TX 77381, USA (1985).
15. J. J. P. Stewart: *J. Comput. Chem.* **10**, 209 (1989).
16. C. K. Johnson: ORTEP II. Report ORNL-5138. Oak Ridge National Laboratory, Tennessee, USA (1976).
17. J. W. Lauher: CHARON. A Graphics Program for Postscript Printers, The Research Foundation of the State University of New York (1989).
18. A. D. Buckingham, P. Claverie, R. Rein and P. Schuster: *Intermolecular Interactions: From Diatomic to Biopolymers*, ed. by B. Pullmann, Wiley, pp. 1–68 (1978).
19. M. Kitagawa, H. Hoshi, M. Sakurai, Y. Inoue, and R. Chûjô: *Bull. Chem. Soc. Jpn.* **61**, 4225 (1988).